

Novel Clinically Relevant Genes in Gastrointestinal Stromal Tumors Identified by Exome Sequencing

Sebastian F. Schoppmann¹, Ursula Vinatzer¹, Niko Popitsch⁵, Martina Mittlböck², Sandra Liebmann-Reindl¹, Gerd Jomrich¹, Berthold Streubel³, and Peter Birner⁴

Abstract

Purpose: Chromosomal gains and losses resulting in altered gene dosage are known to be recurrent in gastrointestinal stromal tumors (GIST). The aim of our study was the identification of clinical relevant genes in these candidate regions.

Material and Methods: A cohort of 174 GIST was investigated using DNA array ($n = 29$), FISH ($n = 125$), exome sequencing ($n = 13$), and immunohistochemistry ($n = 145$).

Results: Array analysis revealed recurrent copy number variations (CNVs) of chromosomal arms 1p, 1q, 3p, 4q, 5q, 7p, 11q, 12p, 13q, 14q, 15q, and 22q. FISH studies of these CNVs showed that relative loss of 1p was associated with shorter disease-free survival (DFS). Analysis of exome sequencing concentrating on target regions showing recurrent CNVs revealed a median number of 3,404 (range 1,641–13,602) variants (SNPs, insertions, deletions) in each tumor minus paired blood sample; variants in at least three samples were observed in 37 genes. After further analysis, target genes were reduced to 10 in addition to *KIT* and *PDGFRA*. Immunohistochemical investigation showed that expression of *SYNE2* and *DIAPH1* was associated with shorter DFS, expression of *RAD54L2* with shorter and expression of *KIT* with longer overall survival.

Conclusion: Using a novel approach combining DNA arrays, exome sequencing, and immunohistochemistry, we were able to identify 10 target genes in GIST, of which three showed hitherto unknown clinical relevance. Because the identified target genes *SYNE2*, *MAPK8IP2*, and *DIAPH1* have been shown to be involved in MAP kinase signaling, our data further indicate the important role of this pathway in GIST. *Clin Cancer Res*; 19(19); 5329–39. ©2013 AACR.

Introduction

Gastrointestinal stromal tumors (GIST) are the most common mesenchymal tumors of the gastrointestinal tract (1). They are thought to arise from Cajal cells or their precursors and characteristically harbor gain of function mutations in *KIT* leading to constitutive activation of the *KIT* receptor (2).

An alternative mutation in a related tyrosine kinase, *PDGFRA*, is found in 35% of *KIT* mutation negative GIST (3, 4). Imatinib mesylate is a molecularly targeted drug

known to inhibit both *KIT* and *PDGFRA* receptors and used in the treatment of recurrent and metastatic GIST or GIST with high risk of progression (5). Effectiveness of imatinib mesylate depends on the mutational status of *KIT* and *PDGFRA* (3). In contrast to metastatic GIST, radical surgery seems to be the best treatment option for localized tumors (6). The recurrence rate after radical surgery seems to depend mainly on tumor localization, size, and mitotic activity and ranges between 5% and 75% with a poor clinical outcome in relapsed patients (7, 8). Current classifications take into account tumor size, mitotic rate, and tumor location but do not include mutational data nor protein expressions of tumor cells (9–11).

The discovery of *KIT* and *PDGFRA* activating mutations in the majority of GIST represents a significant progress in understanding their biological behavior. Although further molecular mechanisms underlying the development and progression of GIST are not fully understood, they are necessary due to the wide range of clinical behavior. Chromosomal gains and losses resulting in altered gene dosage are known to be recurrent in GIST and believed to have a role in the molecular pathogenesis of these tumors (12–19). Nevertheless, the target genes remain to be identified within these regions.

Authors' Affiliations: ¹Department of Surgery; ²Center for Medical Statistics, Informatics, and Intelligent Systems; ³Department of Obstetrics and Gynecology and Core Unit Next Generation Sequencing; ⁴Clinical Institute of Pathology, Medical University of Vienna; and ⁵Center for Integrative Bioinformatics Vienna (CIBIV), Max F Perutz Laboratories, University of Vienna & Medical University of Vienna, & Faculty of Computer Science, University of Vienna, Vienna, Austria

Note: Supplementary data for this article are available at Clinical Cancer Research Online (<http://clincancerres.aacrjournals.org/>).

Corresponding Author: Berthold Streubel, Department of Obstetrics and Gynecology, Medical University of Vienna, Währinger Gürtel 18-20, A-1090 Vienna, Austria. Phone: 43-1404002821; Fax: 43-1404002862; E-mail: berthold.streubel@meduniwien.ac.at

doi: 10.1158/1078-0432.CCR-12-3863

©2013 American Association for Cancer Research.

Translational Relevance

Gastrointestinal stromal tumors (GIST) are the most common mesenchymal tumors of the gastrointestinal tract, characterized by uncertain clinical behavior. In addition to KIT, there is a strong need for further therapeutic targets in GIST. Using a technical approach combining DNA array analysis, next generation exome sequencing, and immunohistochemistry, we were able to identify 10 novel, frequently mutated genes in GIST, of which 3 showed hitherto unknown clinical relevance. Because a part of the identified target genes has been shown to be involved in MAP kinase signaling, our data further indicate the important role of this pathway in GIST. So the inclusion of MAP kinase pathway parameters in future clinical studies might be of potential benefit for patients as selective inhibitors are available.

The aim of our study was the identification of putative prognostic markers within the regions with recurrent gains or losses. We measured copy number variations (CNVs) and defined exact chromosomal breakpoints for the most common alterations in GIST. CNVs were screened in a large single-center cohort of GIST and correlated with clinical outcome. Exome sequencing identified mutated candidate genes in the regions of interest, and protein products of identified target genes were investigated immunohistochemically in our large single-center cohort of GIST.

Patients and Methods

Patients

We studied a total of 174 cases of GIST treated at the Medical University of Vienna between August 1992 and February 2011 in this retrospective observational study. Clinical data and follow-up were available for 145 of 174 cases. All cases were restaged according to UICC TNM classification of malignant tumors 7th edition and risk was evaluated according to Fletcher and Miettinen (9–11). As this cohort of patients has been used in several previous studies, clinical data in correlation with known risk factors have been reported previously, as well as the results of the sequence analysis about mutations of *KIT* (exons 9, 11, 13, and 17) and *PDGFRA* (exons 12 and 18; refs. 20–22). Tissue microarrays were established for immunohistochemical screening in all 145 cases. FISH was conducted on tissue microarrays of paraffin-embedded tissue in 125 of 145 cases. Apart from the 145 cases with clinical follow-up data and paraffin-embedded tissue available, further 29 GIST cases were identified with fresh-frozen tumor material suitable for microarray analysis and next generation sequencing. Tumor purity was at least 90% in samples used in all 29 cases. Institutional review board approval was obtained.

Microarray analysis

High-quality genomic DNA was obtained from 29 fresh-frozen tumor samples using the DNeasy Blood & Tissue Kit (Qiagen) and subjected to microarray analysis using the commercially available Affymetrix Genome-Wide Human SNP Array 6.0 (Affymetrix Inc.) following the protocols provided by the manufacturer. Data analysis was conducted with Affymetrix Genotyping Console 3.0.1 using the Birdseed Algorithm and Affymetrix Chromosome Analysis Suite 1.01 at a resolution of 500 kb. Genome annotations applied in data analysis referred to the human reference assembly GRCh37/hg19 as provided by the Affymetrix annotation file release na31. The reference model file used for data normalization with GTC was generated from 39 healthy control individuals. CNVs showing an overlap greater than 80% with benign CNVs of the Database of Genomic Variants (<http://projects.tcag.ca/variation/>) were excluded from our analysis.

Somatic CNV status of matching tumor-blood/normal tissue samples was used to confirm gains and losses using TaqMan real-time PCR or FISH.

FISH analysis

Tissue microarrays from 125 GIST paraffin-embedded samples were used for FISH. Screening for CNVs was conducted using commercially available probes for *TP73* (chromosomal band 1p36), *ABL2* (1q25), *CCND1* (11q13), *DLEU* (13q14), *IGH* (14q32), *SNRPN* (15q11), and *CLTCL1* (22q11.2; Abbott and Kreatech). FISH procedures and analyses were conducted according to standard protocols.

Immunohistochemical analysis

Tissue microarrays containing 145 GIST samples were used for evaluation of protein expression. Supplementary Table S2 summarizes the antibodies used.

Immunohistochemical analysis was conducted using a Benchmark Ultra Immunostainer (Ventana), except for expression of RB, where a DAKO autostainer (DAKO) was used. A specimen was considered to be positive if the vast majority of cells (>80%) showed distinct staining. The number of cases differed between antibodies due to the use of tissue microarrays, and for investigation of FLT4 and AP1B1 the blocks had to be recut, resulting in the loss of several spots.

Exome studies

Thirteen of the 29 GIST of the microarray study were subjected to high-throughput sequencing. In all these cases, matched control DNA obtained from the peripheral blood or normal gastric tissue of patients were sequenced in parallel. Exome enrichment was conducted using the TruSeq sample prep (Illumina). Sequencing was conducted on a HiSeq 2000 (Illumina). All datasets were aligned with BWA v0.6.1-r104 against the human g1k v37 genome using standard parameters. We conducted INDEL realignment with GATK v1.4, removed PCR duplicates using Picard v1.56 and recalibrated per-base quality values using GATK. Variants were then called and filtered using 2 independent pipelines based on GATK's UnifiedGenotyper (here SNPs

and INDELs were filtered separately) and SAMTOOLS, respectively. The variant sets were then merged and we selected all variants from the matched normal-tumor pairs that were either unique in the tumor sample or changed their predicted genotype from being heterozygous in the normal sample to being homozygous in the cancer sample. We annotated these candidate variants using SnpEff 2.0.4 RC1 and predicted the possible effect of a variant (e.g., silent/nonsilent/nonsense mutation) using the NCBI Reference Sequence (RefSeq) gene annotations. We further determined whether a variant was already contained in the dbSNP TSI (Toscani in Italia) dataset. Candidate variants were further annotated using polyphen2 and finally manually filtered and inspected using IGV. Genes were compared with PubMed, Gene database, and the CancerGenes database for gene selection and prioritization. Variants in candidate genes were confirmed by Sanger sequencing in all tested cases.

Statistical analysis

Categorical data were described with absolute and relative frequencies. Corresponding 95% confidence intervals (95% CI) were calculated according to the method of Wilson. Group differences were tested by χ^2 test or by Fisher exact test in the case of sparse data. Continuous data are described with median, minimum, and maximum. Differences between 2 groups for continuous and ordinal data were tested by Mann-Whitney *U* test.

Disease-free survival (DFS) was defined from the day of surgery until first evidence of progression of disease if complete surgical resection was possible. Patients showing advanced disease at time of initial diagnosis were excluded from analysis of DFS. Overall survival (OS) was defined as the time from primary surgery to patients' death. Survival data were graphically presented by Kaplan-Meier graphs and/or described by survival at predefined time points. Group differences are tested by the log-rank test. Cox regression models were used to estimate the effect of the expression of proteins adjusted for patients' age (<60 vs. \geq 60) and risk according to Fletcher's score. Group differences are quantified with HR and corresponding 95% CIs. Proportional hazards assumptions were graphically checked by log-minus-log plots in stratified Cox regression models for every variable in the Cox model separately.

A two-tailed *P*-value of ≤ 0.05 was considered as significant. SPSS 20.0 (IBM) was used for all calculations. For exploratory purposes, all *P* values together were also adjusted to result in a false discovery rate (FDR) of 0.05 as described by Benjamini and Hochberg (23). Significant results after FDR-adjustment are marked by "a".

Results

Clinical characteristics of patients

Table 1 summarizes the clinical data of the 145 patients with available clinical and follow up data. In brief, 94 GIST (64.8%) were of gastric localization (64.8%), 92 (63.4%) showed a *KIT* mutation, and 21 (14.5%) a *PDGFRA* muta-

tion. All patients underwent initial surgical treatment; 25 patients received adjuvant imatinib mesylate. Median observation time was 37 ± 3 (SE) months. Although 7 patients showed advanced stage disease already at time of diagnosis, and no complete surgical removal of the GIST was possible, 24 patients experienced recurrent disease, and 12 died.

Recurrent chromosomal gains and losses

The microarray technology was conducted to define recurrent chromosomal regions and to determine exact breakpoints in 29 GIST tumors. Although the microarray platform used allows for the detection of CNVs down to 50 kb or smaller, we aimed to assess the minimal region of overlap of recurrent genomic regions that are known to be much larger. Therefore, we used a resolution of 500 kb and found 114 CNVs (43 gains and 71 losses) in the 29 tumor samples altogether (median number of CNVs/sample). We compared the CNVs between the 29 cases and defined rearrangements as recurrent when observed in at least 3 cases. Eighty-five of the 114 CNVs (75%) were located within recurrent rearrangements and included losses of chromosomal arms 1p ($n = 13$), 3p ($n = 4$), 13q ($n = 5$), 14q ($n = 17$), 15q ($n = 7$), and 22q ($n = 11$) as well as gains of chromosomal arms 1q ($n = 3$), 4q ($n = 6$), 5q ($n = 8$), 7p ($n = 3$), 11q ($n = 4$), and 12p ($n = 3$; Table 2).

CNVs were confirmed in all samples by FISH and TaqMan assays (1p: Hs05732825_cn; 3p: Hs01499513_cn; 5q: Hs02944177_cn; 11q: Hs06329804_cn; 13q: Hs07026395_cn; 14q: Hs02834878_cn; 15q: Hs05354966_cn; 22q: Hs01356996_cn).

A detailed list of CNVs is provided in Table 2. In conclusion, we found that the majority of chromosomal imbalances were recurrent, indicating that candidate genes relevant for GIST pathogenesis are located in these regions.

Gains and losses in correlation with clinico-pathologic data

In a next step, we investigated if recurrent CNVs are of prognostic relevance. Seven of the 12 regions (1p, 1q, 11q, 13q, 14q, 15q, and 22q) were investigated on tissue microarrays containing 125 GIST tumors. About the remaining 5 regions, commercially available probes did not provide reliable signals on the tissue microarrays.

Results about frequencies of losses and gains are summarized in Supplementary Table S1 and were comparable to DNA microarrays. CNV status of investigated regions was correlated with clinical risk factor, tumor localization, DFS, OS, and *KIT* and *PDGFRA* mutations status.

FISH for chromosome 1p was successful in 119 samples. Loss of 1p (Fig. 1) was seen in 11 samples (9.2%; 95% CI, 5.2–15.8%), in 5 additional cases, a chromosomal imbalance between 1p and 1q was observed ($5 \times 1p/1q+$). When investigating the 16 cases (13.4%; 95% CI, 8.5–20.7%) with relative imbalance of 1p against all other cases, no association with clinical risk factor was seen either, but these cases showed a significantly shorter DFS (5 years DFS rate: 40.4% $\pm 17\%$ SE vs. 84.6% $\pm 4.4\%$ SE, $P = 0.012$, log-rank test) but

Table 1. Clinico-pathologic data of 145 GIST patients included into this study

Factor	Number of cases	5 Years disease-free survival rate \pm SE	5 years overall survival rate \pm SE
Localization		$P < 0.001^a$	$P > 0.05$
Gastric	94 (64.8%)	89.8 \pm 4.3%	–
Duodenum	6 (4.1%)	100%	–
Small intestine	27 (18.6%)	62.2 \pm 10.1%	–
Rectum	3 (2.1%)	100%	–
Other	15 (10.3%)	45.1 \pm 14.9%	–
Risk Fletcher		$P = 0.001^a$	$P < 0.001^a$
Very low	16 (11%)	87.5 \pm 11.7%	100%
Low	50 (34.5%)	93.9 \pm 4.2%	95.5 \pm 4.4%
Intermediate	32 (22.1%)	79 \pm 8.6%	96.4 \pm 3.5%
High	47 (32.4%)	54.8 \pm 9.7%	73.8 \pm 7.8%
Risk Miettinen		$P < 0.001^a$	$P < 0.001^a$
None	18 (12.4%)	90 \pm 9.5%	100%
Very low	38 (26.2%)	96.3 \pm 3.6%	93.8 \pm 6.1%
Low	28 (19.3%)	77 \pm 10.7%	95.8 \pm 4.1%
Moderate	17 (11.7%)	84.6 \pm 10%	100%
High	29 (20%)	59.9 \pm 12.4%	65.5 \pm 9.7%
Insufficient data	15 (10.3%)	45.1 \pm 14.9%	83.3 \pm 15.2%
Staging UICC		$P < 0.00^a$	$P > 0.05$
pT1	19 (13.1%)	90 \pm 9.5%	–
pT2	65 (44.8%)	84.5 \pm 6.2%	–
pT3	40 (27.6%)	73.6 \pm 8.9%	–
pT4	21 (14.5%)	50.5 \pm 12.9%	–
Mitotic rate UICC		$P = 0.001^a$	$P < 0.001^a$
Low	96 (66.2%)	87.1 \pm 4.5%	96.7 \pm 2.4%
High	49 (33.8%)	58.9 \pm 8.9%	75.8 \pm 7.1%
Synchronous metastases		$P = 0.003^a$	$P < 0.001^a$
No	131 (90.3%)	80.7 \pm 4.3%	94.6 \pm 2.7%
Yes	14 (9.7%)	47.3 \pm 19%	51.3 \pm 12.5%
<i>KIT</i> mutation		$P > 0.05$	$P > 0.05$
No	53 (36.6%)	–	–
Yes	92 (63.4%)	–	–
<i>PDGFRA</i> mutation		$P > 0.05$	$P > 0.05$
No	124 (85.5%)	–	–
Yes	21 (14.5%)	–	–

^aSignificant results after FDR adjustment.

not OS (Fig. 2). A significant association of relative loss of 1p with localization of the GIST was found ($P = 0.001^a$, χ^2 test). So of 75 gastric GIST, only 4 (5.3%; 95% CI, 5.2–33.4%) showed relative loss of 1p, but 9 of 28 (32.1%; 95% CI, 17.9–50.7%) of small intestinal GIST.

FISH for 15q was successful in only 73 samples, and a significant association of 15q deletion with tumor localization was seen ($P < 0.001^a$, Fisher exact test), because only 2 of 46 gastric (4.4%; 95% CI, 1.2–14.5%) GIST showed 15q deletion, but 8 of 17 (47.1%; 95% CI, 26.2–69%) small intestinal GIST.

FISH for 22q was successful in only 75 GIST, and 22q deletion correlated with gastric localization [$P = 0.01$, χ^2 test; 7 of 48 (14.6%; 95% CI, 7.3–27.2%) gastric GIST, vs. 8

of 18 (44.4%; 95% CI, 24.6–66.3%) small intestinal GIST]. Deletion of 22q correlated with the presence of *KIT* mutations. Although in GIST without *KIT* mutation ($n = 28$), only 3 cases (10.7%; 95% CI, 3.7–27.2%) showed a 22q deletion, there were 15 of 47 (32%; 95% CI, 20.4–46.2%) GIST with *KIT* mutation ($P = 0.038$, χ^2 test).

Candidate genes within gains and losses

In a next step, we compared the recurrent CNVs that were observed in at least 3 cases (i.e., >10% of total cases) and defined minimal regions of overlap shared by all aberrant cases. The results are listed in Table 2. The size of the minimal regions of interest and consecutively the number of genes were too large to identify relevant candidates for the

Table 2. Copy number variations assessed by DNA array ($n = 29$)

Chromosome arm	Type of CNV	Cases (n/%; 95% CI)	ROI Start bp	ROI End bp	Size (Mb)
1p	Loss	13 (45%; 95% CI, 28–63%)	5657217	16851502	11.2
3p	Loss	4 (19%; 95% CI, 6–31%)	47478496	50156251	2.7
13q	Loss	5 (17%; 95% CI, 8–35%)	45307552	49798504	4.5 ^b
14q	Loss ^a	17 (59%; 95% CI, 41–75%)	26370859	28652135	2.3
			41327139	46436189	5.1
			54142190	106897379	52.8
15q	Loss	7 (24%; 95% CI, 12–42%)	49340635	56142902	6.8
22q	Loss	11 (38%; 95% CI, 23–56%)	28772816	51134186	22.4
1q	Gain	3 (10%; 95% CI, 5–33%)	118649839	249224376	232.4
4q	Gain	6 (21%; 95% CI, 10–38%)	52920476	56180478	3.3 ^c
5q	Gain	8 (28%; 95% CI, 15–46%)	120645755	180645101	60.0
7p	Gain	3 (10%; 95% CI, 5–33%)	7058423	62706404	55.7
11q	Gain	4 (19%; 95% CI, 6–31%)	78846125	134944770	56.1
12p	Gain	3 (10%; 95% CI, 5–33%)	479074	15635796	15.2

ROI (region of interest) denotes minimal region of overlap, genome annotations applied in data analysis refer to the human reference assembly GRCh37/hg19.

^aThe minimal region of overlap on chromosome 14 comprised 3 regions with a total size of 60.2 Mb.

^b*RB1* is located within the minimal region of overlap.

^c*KIT* and *PDGFRA* are located within the minimal region of overlap, respectively.

majority. Interestingly, the most frequent gain comprised a small region on chromosome 4 that included *KIT* and *PDGFRA*. Furthermore, *RB1*, which was recently reported to be a strong predictor of clinical outcome in GIST, was located in the deleted small region of overlap on chromosome 13. We concluded that our strategy identified successfully the 2 most prominent genes in GIST, that is *KIT* and *PDGFRA*, within our regions of interest. Nevertheless, the candidate remained elusive for the other regions.

Exome sequencing for the identification of novel candidate genes

Exome sequencing was conducted to identify putative novel candidate genes within the defined regions of interest as outlined in Table 2. We compared tumors with the matched constitutional genomes of 13 patients. The median overall number of variants/exome was 50,625 (range 38,365–58,258) per exome (Supplementary Table S3), the median number of variants (SNPs, insertions, deletions) present in tumor minus paired blood sample was 3,404 (range 1,641–13,602; Supplementary Table S4). Intergenic and intronic variants were excluded and annotation by snpEff reduced the average number from 3,404 to 1,764 (range 1,012–7,300). These variants included the switch of heterozygous mutations to homozygous mutations. Variants were considered only when they were stop mutations, splice site mutations, frame shift mutations, or missense mutations with potential pathogenic at *in silico* prediction. In a next step we looked for genes with recurrent variants in at least 3 patients. Recurrent variants were found in 37 genes and listed in Table 3. Sanger sequencing confirmed the variants in all tested cases. Furthermore, we compared the

37 genes with the Cancer Genes Database, the Gene Database, and GIST publications. Results are listed in Table 3. This strategy reduced the number of candidate genes to 3 or less per region. As expected *KIT*, *PDGFRA*, and *RB1* were among these cases. In addition, we searched for potential interactions between the 37 genes and found positive matches between *DIAPH1* and *AP1B* as well as *MAPK8IP2* and *SYNE2*.

Protein expression in correlation with risk factors

Eleven candidate genes were selected for immunohistochemical evaluation (Table 4 and Supplementary Table S2). Table 4 shows the number of GIST samples investigated, the primary staining pattern, and the number of positive cases for each antibody. Figure 1 gives samples of immunostaining. Gene mutation status has been shown to be linked to protein expression in a variety of human genes, but because protein overexpression might indicate loss of function (e.g., *P53*; ref. 24) as well as gain of function (*KIT*, *ALK*; refs. 25, 26), protein expression was scored as positive versus negative without any hypothesis about the type of altered gene function.

Expression of *RBM5*, *RB*, *UBPY/USP8*, *GTSE1*, *MAPK8IP2*, *APIB1*, and *FLT4* was not associated with risk according to Fletcher, Miettinen, or UICC staging and grading, DFS or OS or metastases at time of diagnosis (Table 4). *RAD54L2* expression was associated with higher risk according to Fletcher (median high vs. intermediate risk; $P = 0.033$; Mann–Whitney U test) and higher UICC staging (median pT3 vs. pT2; $P = 0.032$; Mann–Whitney U test). Expression of *RAD54L2* was associated with shorter OS (5 years OS rate: $80.8\% \pm 12.2\%$ SE vs. $93.7\% \pm 3.2\%$ SE, $P = 0.042$, log-rank

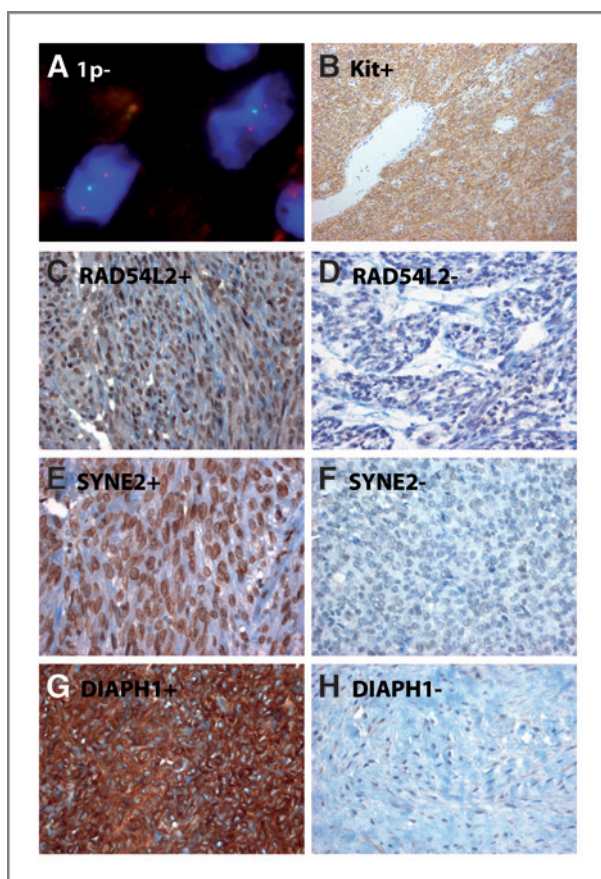


Figure 1. Samples of FISH and immunostaining. A, GIST with loss of 1p at FISH. Original magnification $\times 1,000$. B, GIST positive for KIT. Original magnification $\times 100$. C, GIST positive for RAD54L2. Original magnification $\times 400$. D, GIST negative for RAD54L2. Original magnification $\times 400$. E, GIST positive for SYNE2. Original magnification $\times 400$. F, GIST negative for SYNE2. Original magnification $\times 400$. G, GIST positive for DIAPH1. Original magnification $\times 400$. H, GIST negative for DIAPH1. Original magnification $\times 400$.

test; Fig. 2), but not with shorter DFS. High SYNE2 expression was associated with high mitotic rate according to UICC (60% vs. 26.9%; $P < 0.001^a$, χ^2 test) and with higher risk according to Fletcher and Miettinen ($P = 0.044$ and 0.031 , respectively; Mann–Whitney U tests) and shorter DFS (5 years DFS rate: $43.1\% \pm 14.1\%$ SE vs. $87.2\% \pm 4.2\%$ SE, $P = 0.001^a$, log-rank test) but not OS ($P = 0.06$, log-rank test; Fig. 2). In addition, SYNE2 expression was less common in gastric (7 of 80) than in small intestinal GIST (9 of 22; $P = 0.006^a$, χ^2 test).

A correlation of SYNE2 and MAPK8IP2 protein expression was seen ($P = 0.014$; χ^2 test), but not between DIAPH1 and AP1B1 due to the overexpression of the latter in all samples.

GTSE1 expression was more common in small intestinal (7 of 22) than gastric (5 of 69) GIST ($P = 0.013$, χ^2 test).

Kit expression correlated with lower risk according to Fletcher (median intermediate vs. high risk, $P = 0.035$, Mann–Whitney U test), and lower UICC staging (median pT2 vs. pT3; $P = 0.007$, Mann–Whitney U test). Expression of Kit was associated with longer OS (5 years OS rate: 94.5%

$\pm 2.4\%$ SE vs. $67.2\% \pm 16.5\%$ SE, $P = 0.011$, log-rank test; Fig. 2), but not DFS. The presence of a *KIT* mutation had no influence on DFS or OS ($P > 0.05$, log-rank test). A strong correlation of DIAPH1 expression with risk according to Fletcher (median intermediate vs. low risk, $P < 0.001^a$, Mann–Whitney U test), Miettinen (median moderate vs. very low, $P < 0.001^a$, Mann–Whitney U test), and UICC staging (median pT3 vs. pT2, $P < 0.001^a$, Mann–Whitney U test) was seen. In addition, strong DIAPH1 expression was associated with high mitotic rate according to UICC (45.1% vs. 15.6%, $P = 0.001^a$, χ^2 test) and small intestinal localization (17 of 30 vs. 26 of 74 in gastric GIST; $P = 0.043$, χ^2 test). Expression of DIAPH1 was associated with shorter DFS (5 years DFS rate: $57.3\% \pm 10.2\%$ SE vs. $92.8\% \pm 4.1\%$ SE months, $P = 0.007$, log-rank test; Fig. 2), but not with shorter OS ($P > 0.05$, log-rank test).

In a Cox regression model adjusting for patients' age and Fletchers score, SYNE2 expression was still associated with shorter DFS ($P = 0.046$; HR = 2.85; 95% CI, 1.02–7.97), and expression of DIAPH1 with longer OS ($P = 0.030$; HR = 0.16; 95% CI, 0.03–0.84).

When also including synchronous metastases, adjuvant administration of imatinib mesylate, *KIT* and *PDGFRA* mutations into the regression models, SYNE2 expression remained an independent prognostic factor for shorter DFS ($P = 0.012$; HR = 3.92; 95% CI, 1.35–11.42), whereas no relevance of *KIT* and *PDGFRA* mutations or adjuvant imatinib mesylate administration was observed.

A prognostic relevance of DIAPH1 expression on OS ($P = 0.042$; HR = 0.16; 95% CI, 0.03–0.95) was seen after introduction of *KIT* and *PDGFRA* mutations into the regression model, but this was not evident any more ($P = 0.077$) after inclusion of imatinib mesylate administration and synchronous metastases. *KIT* and *PDGFR* mutations showed again no prognostic relevance.

No significant additional effect of RAD54L2 or Kit expression was seen to explain DFS and OS additional to the effect of patients' age and Fletcher score ($P > 0.05$).

A combination of combined SYNE2 and DAPH1 expression showed a prognostic relevance for DFS in univariate analysis (5 years DFS rate: $25\% \pm 19.4\%$ SE vs. $85.7\% \pm 4.4\%$ SE, $P = 0.001^a$, log-rank test; Fig. 2) as well as after adjustment for patients' age and Fletchers score in a multivariate Cox regression ($P = 0.025$; HR = 3.58; 95% CI, 1.17–10.90). The prognostic relevance was also seen ($P = 0.01$; HR = 4.94; 95% CI, 1.17–16.55) when introducing adjuvant imatinib mesylate, synchronous metastases, *KIT* and *PDGFRA* mutations (in addition to age and Fletcher score) into the regression model.

The combination of SYNE2 and RAD54L2 expression, which was only evident in 2 patients, was associated with shorter OS in univariate analysis ($P < 0.001^a$, log-rank test), but did not reach significance in multivariate analysis of OS.

The combination of expression of target genes with high UICC mitotic rate delivered no additional prognostic information ($P > 0.05$, Cox regression).

No protein was associated with the presence of metastases already at time of surgery ($P > 0.05$, χ^2 test). Kit protein

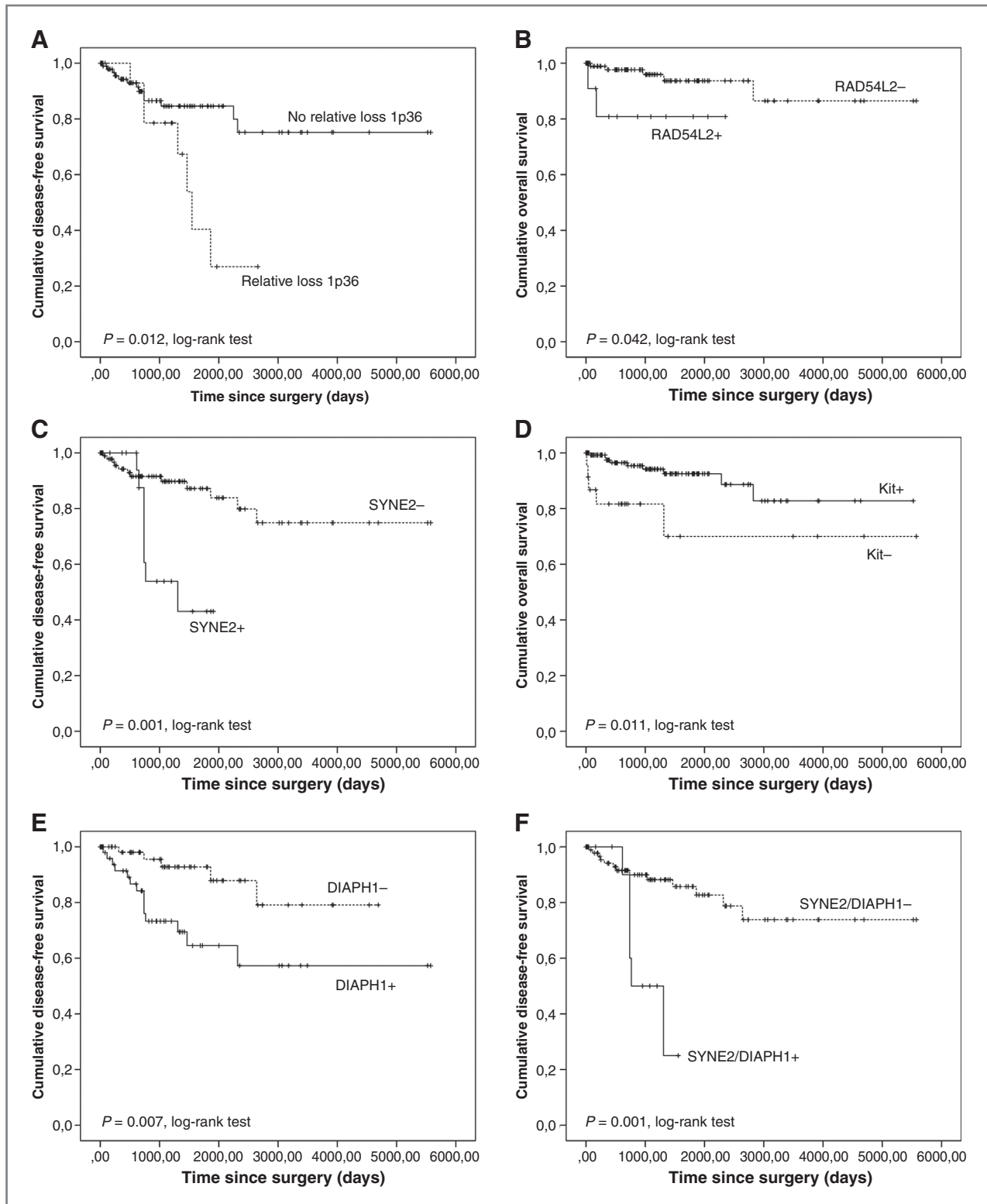


Figure 2. Kaplan-Meier curves of DFS and OS, ticks indicate censored observations. A, DFS according to relative loss of 1p. B, OS according to RAD54L2 expression. C, DFS according to SYNE2 expression. D, OS according to Kit expression. E, DFS according to DIAPH1 expression. F, DFS according to a combination of SYNE2 and DIAPH1 expression (SYNE2/DIAPH1+) versus all other cases (SYNE2/DIAPH1-).

Table 3. Results of exome sequencing in 13 patients

Region of interest	Type defined by microarray	Number of genes with variants	Genes with recurrent variations	Number of cases (95% CI)	Potentially oncogenic (according to Cancer genes)	PubMed Search: Gene AND GIST	Potential oncogenic according to Gene Database
1p	Loss	48	<i>GPR153</i>	4 (31%; 95% CI, 13–58%)	No	No	No
			<i>LOC440563</i>	4 (31%; 95% CI, 13–58%)	No	No	No
			<i>PRAMEF19</i>	4 (31%; 95% CI, 13–58%)	No	No	No
			<i>CROCC</i>	5 (39%; 95% CI, 18–65%)	No	No	Yes
			<i>PRAMEF1</i>	6 (46%; 95% CI, 23–71%)	No	No	Yes
			<i>HNRNPCL1</i>	7 (54%; 95% CI, 29–77%)	No	No	Yes
			3p	Loss	33	<i>ALS2CL</i>	3 (23%; 95% CI, 8–50%)
<i>COL7A1</i>	3 (23%; 95% CI, 8–50%)	No				No	No
<i>LAMB2</i>	3 (23%; 95% CI, 8–50%)	No				No	Yes
<i>MST1</i>	3 (23%; 95% CI, 8–50%)	No				No	Yes
<i>RBM5^a</i>	3 (23%; 95% CI, 8–50%)	Yes				No	Yes
<i>RAD54L2^a</i>	4 (31%; 95% CI, 13–58%)	Yes				No	Yes
13q	Loss	9	<i>FAM194B</i>	4 (31%; 95% CI, 13–58%)	No	No	Yes
			<i>RB1^a</i>	3 (23%; 95% CI, 8–50%)	Yes	Yes	Yes
14q	Loss	64	<i>SYNE2^{a,b}</i>	3 (23%; 95% CI, 8–50%)	No	No	Yes
			<i>GALC</i>	3 (23%; 95% CI, 8–50%)	No	No	No
			<i>DYNC1H1</i>	5 (39%; 95% CI, 18–65%)	No	No	No
			<i>AHNAK2</i>	6 (46%; 95% CI, 23–71%)	No	No	No
15q	Loss	12	<i>MYO5A</i>	3 (23%; 95% CI, 8–50%)	No	No	No
			<i>USP8^a</i>	5 (39%; 95% CI, 18–65%)	No	No	Yes
22q	Loss	80	<i>AP1B1^c</i>	3 (23%; 95% CI, 8–50%)	No	No	Yes
			<i>NEFH</i>	3 (23%; 95% CI, 8–50%)	No	No	No
			<i>SEC14L4</i>	3 (23%; 95% CI, 8–50%)	No	No	No
			<i>RFPL3</i>	3 (23%; 95% CI, 8–50%)	No	No	No
			<i>GTSE1^a</i>	3 (23%; 95% CI, 8–50%)	Yes	No	Yes
			<i>MAPK8IP2^{a,b}</i>	3 (23%; 95% CI, 8–50%)	Yes	No	Yes
			<i>TUBGCP6</i>	4 (31%; 95% CI, 13–58%)	No	No	No
4q	Gain	4	<i>PDGFRA</i>	3 (23%; 95% CI, 8–50%)	Yes	Yes	Yes
			<i>KIT^a</i>	6 (46%; 95% CI, 23–71%)	Yes	Yes	Yes
5q	Gain	100	<i>DIAPH1^{a,c}</i>	3 (23%; 95% CI, 8–50%)	Yes	No	Yes
			<i>FAT2</i>	3 (23%; 95% CI, 8–50%)	Yes	No	Yes
			<i>PCDHB8</i>	3 (23%; 95% CI, 8–50%)	No	No	No
			<i>TCOF1</i>	3 (23%; 95% CI, 8–50%)	No	No	No
			<i>YIPF5</i>	3 (23%; 95% CI, 8–50%)	No	No	No
			<i>C5orf65</i>	4 (31%; 95% CI, 13–58%)	No	No	No
			<i>CDHR2</i>	4 (31%; 95% CI, 13–58%)	No	No	Yes
			<i>F12</i>	4 (31%; 95% CI, 13–58%)	No	No	No
			<i>FLT4^a</i>	4 (31%; 95% CI, 13–58%)	Yes	Yes	Yes

^aProtein expressions were evaluated immunohistochemically and correlated with risk factors.
^bPotential interaction.
^cPotential interaction.

Table 4. Expression of proteins and correlation of overexpression with prognostic parameters

Protein	Number of investigated cases	Primary staining pattern	Positive cases	95% CI	Fletcher risk	Miettinen risk	UICC staging	UICC mitotic rate	Localization	Survival	KIT mutations
RBM5	118	Nucleus	108 (91.5%)	85.1–95.3%	-	-	-	-	-	-	-
RAD54L2	114	Nucleus	11 (9.6%)	5.5–16.5%	Yes	-	Yes	-	-	Shorter OS	-
RB1	106	Nucleus	20 (18.9%)	12.6–27.4%	-	-	-	-	-	-	-
SYNE2	128	Nucleus	23 (18%)	12.3–25.5%	Yes	Yes	-	Yes	Small intestinal	Shorter DFS	-
USP8	120	Cytoplasm	108 (90%)	83.3–94.2%	-	-	-	-	-	-	-
AP1B1	74	Cytoplasm	74 (100%)	95.1–100%	-	-	-	-	-	-	-
GTSE1	119	Cytoplasm	14 (11.8%)	7.1–18.8%	-	-	-	-	Small intestinal	-	-
MAPK8IP2	137	Cytoplasm	69 (50.4%)	42.1–58.6%	-	-	-	-	-	-	-
KIT	145	Cytoplasm	126 (86.9%)	80.4–91.5%	Yes (neg.)	-	Yes (neg.)	-	-	Longer OS	Yes
DIAPH1	119	Cytoplasm	54 (45.4%)	36.7–54.3%	Yes	Yes	Yes	Yes	-	Shorter DFS	-
FLT4	75	Cytoplasm	30 (40%)	29.7–51.3%	-	-	-	-	-	-	-

Abbreviation: neg., negative correlation.

expression was found significantly more often in mutated tumors ($P < 0.001^a$, χ^2 test; 93.5% vs. 74.1%), whereas expression of all other proteins showed no association with *KIT* or *PDGFRA* mutation. A correlation of RB 1 expression with loss at 13q was seen ($P = 0.017$, Fisher exact test), whereas in GIST without nuclear RB1 expression, 24 of 66 (36.4%) showed a deletion on 13q, there were only 1 of 17 (5.9%) in patients positive for RB1 expression. In summary, expression of RAD54L2, SYNE2, KIT, and DIAPH1 correlated with risk factors and survival.

In rearward stepwise Cox regression models of DFS and OS including all relevant parameters, SYNE2 expression ($P = 0-018$; HR = 3.8; 95% CI, 1.26–11.48) remained an independent prognostic factor for DFS and DIAPH1 expression for OS ($P = 0.042$; HR = 0.59; 95% CI, 0.004–0.9) in the last step of the regression models, respectively (Supplementary Table S5).

Discussion

In this study, we combined several techniques to identify putative prognostic factors within genomic GIST target regions. Microarray analysis was used to define minimum regions of interest for 12 recurrent gains or losses, FISH showed prognostic significance of 1p loss. Exome sequencing identified 37 recurrent potential pathogenic variations, and 11 candidates were chosen for immunohistochemical screening and correlation with clinical data. An association with survival was found for RAD54L2, SYNE2, KIT, and DIAPH1 expressions.

KIT is a well-known proto-oncogene in human tumors. Although *KIT* mutations are a common event in GIST, overexpression of *KIT* is observed considerably more often, showing no clear association with mutation status (27, 28).

Generally, overexpression of *KIT* serves as primary biomarker for induction of imatinib therapy (29), whereas the exact mutation status serves only for adjustment of it (30). The general presence of *KIT* mutations does not seem to be associated with worse prognosis in GIST, but deletion of exon 11 is accompanied with shorter survival in untreated patients (31). In contrast, other authors found no prognostic relevance of *KIT* mutations after curative surgical resection of GIST (32). Consensus exists that in patients treated with imatinib mesylate, *KIT* exon 9 mutations or lack of *KIT* mutations are associated with inferior response to imatinib (3, 33). Although many data on immunohistochemical expression of *KIT* as diagnostic and predictive marker for GIST do exist (34), surprisingly few data on the prognostic relevance of *KIT* expression are available: thus, it was not an independent prognostic factor in 95 GIST (32). In our study, *KIT* protein expression was found significantly more often in cases with *KIT* mutation. Lack of *KIT* expression was associated with shorter OS, but because 6 of 19 IHC-negative GIST showed a *KIT* mutation and 5 of 19 a *PDGFRA* mutation at sequencing, and 3 patients received imatinib, this subject deserves further investigation in a more homogenous collective.

Chromosomal gains and losses are consistent findings in GIST. Our data are consistent with previous reports with

losses of 1p, 3p, 13q, 14q, 15q, and 22q and gains of chromosomes 4 and 5 (12–19). Only one previous study of 25 GIST tumors used the same platform and provided comparable high-resolution copy number analysis (17). Regions of interest were investigated for candidate genes by gene expression analyses in that study. This approach failed to identify *PDGFRA* and *KIT* on chromosome 4 and *RB1* on chromosome 13 in contrast to our study using a combination with exome sequencing. About the prognostic relevance of CNVs in GIST, loss of 1p and 15q were reported to be more common in clinically more aggressive GIST (35). Loss of 1p has also been shown to be more common in intestinal GIST, and was associated with a more aggressive clinical course in that study as well (36). In contrast, the pathway characterized by loss of 14q has been suggested to be associated with gastric tumors with stable karyotypes and a more favorable clinical outcome (36). In our study, relative loss of 1p at FISH was significantly associated with GIST of the small bowel and with more aggressive clinical course, which is in good correlation to previous data obtained by comparative genomic hybridization (36). In contrast to the findings by Gunawan and colleagues, no association of 14q deletion with gastric localization or better prognosis was seen in our study (36). Furthermore, we failed to identify loss of *RB1* expression as a prognostically relevant factor. This is in contrast to recent data, where *RB1* was integrated in a genomic index for mitotic checkpoints that was reported as a strong predictor of clinical outcome in GIST (19).

Apart from established candidates for 4q gain (*KIT* and *PDGFRA*) and 13q loss (*RB1*), we were able to provide new candidates in further recurrent regions of interest, and to define target genes in previously known areas of CNVs. *RAD54L2* on chromosomal arm 3p, *DIAPH1* on 5q and *SYNE2* on 14q may be of biological relevance because associations with staging and survival were observed. Although all 3 genes have not been reported in GIST so far, no data at all on *RAD54L2* in human malignant disease exist, and there is only one study about *SYNE2*, where the presence of splice variants was reported in human non-small lung cancer (37). *DIAPH1* is a downstream effector of RhoA, controls actin-dependent processes such as cytokinesis, SRF transcriptional activity, and cell motility (38, 39), and might therefore play a role in human cancer progres-

sion (40). To our knowledge, no *DIAPH1* mutations in human malignant disease have been described previously.

Interestingly, *SYNE2* encodes for a nuclear outer membrane protein and has been shown to play a role in MAP kinase signaling pathways (MAPK1 and MAPK2) in promyelocytic leukemia protein (41). *SYNE2* also interacts with MAPK8IP2, which is one of our candidate genes on chromosomes 22 (42), and a correlation of expression of these 2 proteins was also seen in our study. Interestingly, we found recently that high MAPKAPK2 expression is also a strong prognostic predictor in the GIST cohort investigated in this study (21). Because *DIAPH1* inhibition has also been shown recently to block ERK– phosphorylation (43), our findings indicate that altered MAP kinase signaling seems to be of crucial importance in GIST.

In summary, using high-throughput methods we identified several new candidate genes that may be of pathogenetic and prognostic significance in GIST. Our data indicate that the MAP kinase signaling pathway seems to play an important role in GIST. So the inclusion of MAP kinase pathway parameters in future clinical studies might be of potential benefit for the patients as selective inhibitors are available.

Disclosure of Potential Conflicts of Interest

No potential conflicts of interest were disclosed.

Authors' Contributions

Conception and design: S.F. Schoppmann, B. Streubel, P. Birner

Development of methodology: S.F. Schoppmann, P. Birner

Acquisition of data (provided animals, acquired and managed patients, provided facilities, etc.): S.F. Schoppmann, U. Vinatzer, S. Liebmann-Reindl, G. Jomrich, P. Birner

Analysis and interpretation of data (e.g., statistical analysis, biostatistics, computational analysis): U. Vinatzer, N. Popitsch, M. Mittlböck, B. Streubel, P. Birner

Writing, review, and/or revision of the manuscript: S.F. Schoppmann, N. Popitsch, B. Streubel, P. Birner

Administrative, technical, or material support (i.e., reporting or organizing data, constructing databases): G. Jomrich, B. Streubel

Study supervision: S.F. Schoppmann, P. Birner

Acknowledgments

The authors thank Amy Bruno-Lindner for language editing.

The costs of publication of this article were defrayed in part by the payment of page charges. This article must therefore be hereby marked *advertisement* in accordance with 18 U.S.C. Section 1734 solely to indicate this fact.

Received December 19, 2012; revised August 1, 2013; accepted August 1, 2013; published OnlineFirst August 13, 2013.

References

- Miettinen M, Lasota J. Gastrointestinal stromal tumors—definition, clinical, histological, immunohistochemical, and molecular genetic features and differential diagnosis. *Virchows Arch* 2001;438:1–12.
- Hirota S, Isozaki K, Moriyama Y, Hashimoto K, Nishida T, Ishiguro S, et al. Gain-of-function mutations of c-kit in human gastrointestinal stromal tumors. *Science* 1998;279:577–80.
- Heinrich MC, Corless CL, Demetri GD, Blanke CD, von Mehren M, Joensuu H, et al. Kinase mutations and imatinib response in patients with metastatic gastrointestinal stromal tumor. *J Clin Oncol* 2003;21:4342–9.
- Hirota S, Isozaki K. Pathology of gastrointestinal stromal tumors. *Pathol Int* 2006;56:1–9.
- Joensuu H, Eriksson M, Sundby Hall K, Hartmann JT, Pink D, Schutte J, et al. One vs three years of adjuvant imatinib for operable gastrointestinal stromal tumor: a randomized trial. *JAMA* 2012;307:1265–72.
- Blackstein ME, Blay JY, Corless C, Driman DK, Riddell R, Soulieres D, et al. Gastrointestinal stromal tumours: consensus statement on diagnosis and treatment. *Can J Gastroenterol* 2006;20:157–63.
- DeMatteo RP, Lewis JJ, Leung D, Mudan SS, Woodruff JM, Brennan MF. Two hundred gastrointestinal stromal tumors: recurrence patterns and prognostic factors for survival. *Ann Surg* 2000;231:51–8.
- Rutkowski P, Wozniak A, Debiec-Rychter M, Kakol M, Dziewirski W, Zdzienicki M, et al. Clinical utility of the new American joint committee on cancer staging system for gastrointestinal stromal tumors: current

- overall survival after primary tumor resection. *Cancer* 2011;117:4916–24.
9. Fletcher CD, Berman JJ, Corless C, Gorstein F, Lasota J, Longley BJ, et al. Diagnosis of gastrointestinal stromal tumors: a consensus approach. *Hum Pathol* 2002;33:459–65.
 10. Miettinen M, Lasota J. Gastrointestinal stromal tumors: review on morphology, molecular pathology, prognosis, and differential diagnosis. *Arch Pathol Lab Med* 2006;130:1466–78.
 11. Agaimy A. Gastrointestinal stromal tumors (GIST) from risk stratification systems to the new TNM proposal: more questions than answers? A review emphasizing the need for a standardized GIST reporting. *Int J Clin Exp Pathol* 2010;3:461–71.
 12. Gunawan B, Bergmann F, Hoer J, Langer C, Schumpelick V, Becker H, et al. Biological and clinical significance of cytogenetic abnormalities in low-risk and high-risk gastrointestinal stromal tumors. *Hum Pathol* 2002;33:316–21.
 13. Kim NG, Kim JJ, Ahn JY, Seong CM, Noh SH, Kim CB, et al. Putative chromosomal deletions on 9P, 9Q and 22Q occur preferentially in malignant gastrointestinal stromal tumors. *Int J Cancer* 2000;85:633–8.
 14. Igarashi S, Suzuki H, Niinuma T, Shimizu H, Nojima M, Iwaki H, et al. A novel correlation between LINE-1 hypomethylation and the malignancy of gastrointestinal stromal tumors. *Clin Cancer Res* 2010;16:5114–23.
 15. Wozniak A, Sciot R, Guillou L, Pauwels P, Wasag B, Stul M, et al. Array CGH analysis in primary gastrointestinal stromal tumors: cytogenetic profile correlates with anatomic site and tumor aggressiveness, irrespective of mutational status. *Genes Chromosomes Cancer* 2007;46:261–76.
 16. Assamaki R, Sarlomo-Rikala M, Lopez-Guerrero JA, Lasota J, Andersson LC, Llombart-Bosch A, et al. Array comparative genomic hybridization analysis of chromosomal imbalances and their target genes in gastrointestinal stromal tumors. *Genes Chromosomes Cancer* 2007;46:564–76.
 17. Astolfi A, Nannini M, Pantaleo MA, Di Battista M, Heinrich MC, Santini D, et al. A molecular portrait of gastrointestinal stromal tumors: an integrative analysis of gene expression profiling and high-resolution genomic copy number. *Lab Invest* 2010;90:1285–94.
 18. Meza-Zepeda LA, Kresse SH, Barragan-Polania AH, Bjerkehaugen B, Ohnstad HO, Namlos HM, et al. Array comparative genomic hybridization reveals distinct DNA copy number differences between gastrointestinal stromal tumors and leiomyosarcomas. *Cancer Res* 2006;66:8984–93.
 19. Lagarde P, Perot G, Kauffmann A, Brulard C, Dapremont V, Hosten I, et al. Mitotic checkpoints and chromosome instability are strong predictors of clinical outcome in gastrointestinal stromal tumors. *Clin Cancer Res* 2012;18:826–38.
 20. Schoppmann SF, Berghoff AS, Jesch B, Zacherl J, Nirtl N, Jomrich G, et al. Expression of podoplanin is a rare event in sporadic gastrointestinal stromal tumors and does not influence prognosis. *Future Oncol* 2012;8:859–66.
 21. Birner P, Beer A, Vinatzer U, Stary S, Hoftberger R, Nirtl N, et al. MAPKAP kinase 2 overexpression influences prognosis in gastrointestinal stromal tumors and associates with copy number variations on chromosome 1 and expression of p38 MAP kinase and ETV1. *Clin Cancer Res* 2012;18:1879–87.
 22. Schoppmann SF, Beer A, Nirtl N, Ba-Ssalamah A, Brodowicz T, Streubel B, et al. Downregulation of phosphatidylethanolamine binding protein 1 associates with clinical risk factors in gastrointestinal stromal tumors, but not with activation of the RAF-1-MEK-ETV1 pathway. *Cancer Lett* 2013;335:26–30.
 23. Benjamini Y, Hochberg Y. Controlling the false discovery rate: a practical and powerful approach to multiple testing. *J R Stat Soc* 1995;57:289–300.
 24. Kaserer K, Schmaus J, Bethge U, Migschitz B, Fasching S, Walch A, et al. Staining patterns of p53 immunohistochemistry and their biological significance in colorectal cancer. *J Pathol* 2000;190:450–6.
 25. Rubin BP, Singer S, Tsao C, Duensing A, Lux ML, Ruiz R, et al. KIT activation is a ubiquitous feature of gastrointestinal stromal tumors. *Cancer Res* 2001;61:8118–21.
 26. Mino-Kenudson M, Chirieac LR, Law K, Hornick JL, Lindeman N, Mark EJ, et al. A novel, highly sensitive antibody allows for the routine detection of ALK-rearranged lung adenocarcinomas by standard immunohistochemistry. *Clin Cancer Res* 2010;16:1561–71.
 27. Sciot R, Debiec-Rychter M, Daugaard S, Fisher C, Collin F, van Glabbeke M, et al. Distribution and prognostic value of histopathologic data and immunohistochemical markers in gastrointestinal stromal tumours (GISTs): an analysis of the EORTC phase III trial of treatment of metastatic GISTs with imatinib mesylate. *Eur J Cancer* 2008;44:1855–60.
 28. Zheng S, Chen LR, Wang HJ, Chen SZ. Analysis of mutation and expression of c-kit and PDGFR-alpha gene in gastrointestinal stromal tumor. *Hepatogastroenterology* 2007;54:2285–90.
 29. Joensuu H, Roberts PJ, Sarlomo-Rikala M, Andersson LC, Tervahartiala P, Tuveson D, et al. Effect of the tyrosine kinase inhibitor STI571 in a patient with a metastatic gastrointestinal stromal tumor. *N Engl J Med* 2001;344:1052–6.
 30. Koshenkov VP, Rodgers SE. Adjuvant therapy of gastrointestinal stromal tumors. *Curr Opin Oncol* 2012;24:414–8.
 31. Hou YY, Grabellus F, Weber F, Zhou Y, Tan YS, Li J, et al. Impact of KIT and PDGFRA gene mutations on prognosis of patients with gastrointestinal stromal tumors after complete primary tumor resection. *J Gastrointest Surg* 2009;13:1583–92.
 32. Kern A, Gorgens H, Dittert DD, Kruger S, Richter KK, Schackert HK, et al. Mutational status of KIT and PDGFRA and expression of PDGFRA are not associated with prognosis after curative resection of primary gastrointestinal stromal tumors (GISTs). *J Surg Oncol* 2011;104:59–65.
 33. Debiec-Rychter M, Sciot R, Le Cesne A, Schlemmer M, Hohenberger P, van Oosterom AT, et al. KIT mutations and dose selection for imatinib in patients with advanced gastrointestinal stromal tumours. *Eur J Cancer* 2006;42:1093–103.
 34. Wong NA. Gastrointestinal stromal tumours—an update for histopathologists. *Histopathology* 2011;59:807–21.
 35. Chen Y, Tzeng CC, Liou CP, Chang MY, Li CF, Lin CN. Biological significance of chromosomal imbalance aberrations in gastrointestinal stromal tumors. *J Biomed Sci* 2004;11:65–71.
 36. Gunawan B, von Heydebreck A, Sander B, Schulten HJ, Haller F, Langer C, et al. An oncogenetic tree model in gastrointestinal stromal tumours (GISTs) identifies different pathways of cytogenetic evolution with prognostic implications. *J Pathol* 2007;211:463–70.
 37. Langer W, Sohler F, Leder G, Beckmann G, Seidel H, Grone J, et al. Exon array analysis using re-defined probe sets results in reliable identification of alternatively spliced genes in non-small cell lung cancer. *BMC Genom* 2010;11:676.
 38. Kitzing TM, Sahadevan AS, Brandt DT, Knieling H, Hannemann S, Fackler OT, et al. Positive feedback between Dia1, LARG, and RhoA regulates cell morphology and invasion. *Genes Dev* 2007;21:1478–83.
 39. Narumiya S, Tanji M, Ishizaki T. Rho signaling, ROCK and mDia1, in transformation, metastasis and invasion. *Cancer Metastasis Rev* 2009;28:65–76.
 40. Struckhoff AP, Rana MK, Worthylake RA. RhoA can lead the way in tumor cell invasion and metastasis. *Front Biosci* 2011;16:1915–26.
 41. Warren DT, Tajsic T, Mellad JA, Searles R, Zhang Q, Shanahan CM. Novel nuclear nesprin-2 variants tether active extracellular signal-regulated MAPK1 and MAPK2 at promyelocytic leukemia protein nuclear bodies and act to regulate smooth muscle cell proliferation. *J Biol Chem* 2010;285:1311–20.
 42. Vinayagam A, Stelzl U, Foulle R, Plassmann S, Zenkner M, Timm J, et al. A directed protein interaction network for investigating intracellular signal transduction. *Sci Signal* 2011;4:rs8.
 43. Chaturvedi LS, Marsh HM, Basson MD. Role of RhoA and its effectors ROCK and mDia1 in the modulation of deformation-induced FAK, ERK, p38, and MLC motogenic signals in human Caco-2 intestinal epithelial cells. *Am J Physiol Cell Physiol* 2011;301:C1224–38.

Clinical Cancer Research

Novel Clinically Relevant Genes in Gastrointestinal Stromal Tumors Identified by Exome Sequencing

Sebastian F. Schoppmann, Ursula Vinatzer, Niko Popitsch, et al.

Clin Cancer Res 2013;19:5329-5339. Published OnlineFirst August 13, 2013.

Updated version Access the most recent version of this article at:
[doi:10.1158/1078-0432.CCR-12-3863](https://doi.org/10.1158/1078-0432.CCR-12-3863)

Supplementary Material Access the most recent supplemental material at:
<http://clincancerres.aacrjournals.org/content/suppl/2013/08/13/1078-0432.CCR-12-3863.DC1>

Cited articles This article cites 43 articles, 11 of which you can access for free at:
<http://clincancerres.aacrjournals.org/content/19/19/5329.full#ref-list-1>

Citing articles This article has been cited by 9 HighWire-hosted articles. Access the articles at:
<http://clincancerres.aacrjournals.org/content/19/19/5329.full#related-urls>

E-mail alerts [Sign up to receive free email-alerts](#) related to this article or journal.

Reprints and Subscriptions To order reprints of this article or to subscribe to the journal, contact the AACR Publications Department at pubs@aacr.org.

Permissions To request permission to re-use all or part of this article, use this link
<http://clincancerres.aacrjournals.org/content/19/19/5329>.
Click on "Request Permissions" which will take you to the Copyright Clearance Center's (CCC) Rightslink site.